

# Activation of Cytosolic Phospholipase A<sub>2</sub> Downstream of the Src-Phospholipase D1 (PLD1)-Protein Kinase C $\gamma$ (PKC $\gamma$ ) Signaling Axis Is Required for Hypoxia-induced Pathological Retinal Angiogenesis\*

Received for publication, December 31, 2010, and in revised form, April 29, 2011. Published, JBC Papers in Press, May 2, 2011, DOI 10.1074/jbc.M110.217786

Qihua Zhang<sup>†</sup>, Dong Wang<sup>†</sup>, Nikhlesh K. Singh<sup>†</sup>, Venkatesh Kundumani-Sridharan<sup>†</sup>, Laxmisilpa Gadiparthi<sup>†</sup>, Ch. Mohan Rao<sup>§</sup>, and Gadiparthi N. Rao<sup>†1</sup>

From the <sup>†</sup>Department of Physiology, The University of Tennessee Health Science Center, Memphis, Tennessee 38163 and the <sup>§</sup>Center for Cellular and Molecular Biology, Council of Scientific and Industrial Research, Hyderabad 500007, India

In view of understanding the mechanisms of retinal neovascularization, we had reported previously that vascular endothelial growth factor (VEGF)-induced pathological retinal angiogenesis requires the activation of Src-PLD1-PKC $\gamma$  signaling. In the present work, we have identified cytosolic phospholipase A<sub>2</sub> (cPLA<sub>2</sub>) as an effector molecule of Src-PLD1-PKC $\gamma$  signaling in the mediation of VEGF-induced pathological retinal angiogenesis based on the following observations. VEGF induced cPLA<sub>2</sub> phosphorylation in a time-dependent manner in human retinal microvascular endothelial cells (HRMVECs). VEGF also induced arachidonic acid (AA) release in a dose-, time-, and cPLA<sub>2</sub>-dependent manner. Depletion of cPLA<sub>2</sub> levels inhibited VEGF-induced HRMVEC DNA synthesis, migration, and tube formation. In addition, the exogenous addition of AA rescued VEGF-induced HRMVEC DNA synthesis, migration, and tube formation from inhibition by down-regulation of cPLA<sub>2</sub>. Inhibition of Src, PLD1, or PKC $\gamma$  attenuated VEGF-induced cPLA<sub>2</sub> phosphorylation and AA release. Consistent with these findings, hypoxia induced cPLA<sub>2</sub> phosphorylation and activity in VEGF-Src-PLD1-PKC $\gamma$ -dependent manner in a mouse model of oxygen-induced retinopathy. In addition, siRNA-mediated down-regulation of cPLA<sub>2</sub> levels in the retina abrogated hypoxia-induced retinal endothelial cell proliferation and neovascularization. These observations suggest that cPLA<sub>2</sub>-dependent AA release is required for VEGF-induced Src-PLD1-PKC $\gamma$ -mediated pathological retinal angiogenesis.

Ischemic retinal diseases such as diabetic retinopathy, retinal vein occlusion, and retinopathy of prematurity often lead to retinal neovascularization (1, 2). This pathological retinal angiogenesis, in turn, may cause vitreous hemorrhage, retinal detachment, and/or neovascular glaucoma leading to vision loss (3). Among various growth factors produced by hypoxic retina, vascular endothelial growth factor (VEGF)<sup>2</sup> is a potent

vascular permeability and angiogenic factor (4, 5). VEGF induces angiogenesis via its capacity to stimulate the growth, migration, and tubulogenesis of endothelial cells (ECs) and their permeability (6–8). VEGF mediates its vascular permeability and angiogenic effects via its tyrosine kinase receptors, VEGFR1 and VEGFR2 (9–13). The functional segregation between these two receptors in the mediation of angiogenic effects of VEGF is often tied to their distinct temporal and spatial expression (14). Downstream of these receptors, VEGF has been shown to stimulate Src, phospholipase C $\gamma$  (PLC $\gamma$ ), phosphatidylinositol 3-kinase (PI3K), and mitogen-activated protein kinases (MAPKs) in the mediation of its angiogenic actions (15–18). In understanding the mechanisms of pathological retinal angiogenesis, we have demonstrated that VEGF activates PLD1-PKC $\gamma$  signaling downstream of Src in human microvascular endothelial cells (HRMVECs) as well as in the retina in a mouse model of oxygen-induced retinopathy (OIR) (19). PLDs and PKCs play a role in the regulation of cell migration and proliferation (20–23). It was also reported that VEGF-induced EC proliferation requires PLA<sub>2</sub>, particularly cPLA<sub>2</sub> and iPLA<sub>2</sub> (24, 25). By hydrolyzing glycerophospholipids that contain arachidonic acid (AA) at the sn-2 position, cPLA<sub>2</sub> liberates AA, a substrate for the cyclooxygenase, lipoxygenase, and epoxygenase pathways (26). Moreover, it has been found that whereas omega-3 polyunsaturated fatty acids ( $\omega$ -3 PUFA) decrease angiogenesis,  $\omega$ -6 PUFA enhance neovascularization (27, 28). However, it was not known up to now how these various signaling events targeting membrane phospholipids are integrated in the mediation of angiogenesis.

Because  $\omega$ -6 PUFA influence angiogenesis and PLA<sub>2</sub> play a rate-limiting role in AA release, we asked the question whether the cPLA<sub>2</sub>-AA axis plays a role in VEGF-induced pathological retinal angiogenesis. Therefore, the purpose of this study is to find the role of cPLA<sub>2</sub> in pathological retinal angiogenesis and its spatial relationship to Src-PLD1-PKC $\gamma$  signaling. Our studies revealed that VEGF activates cPLA<sub>2</sub> downstream of Src,

\* This work was supported, in whole or in part, by National Institutes of Health Grant EY014856 from NEI (to G. N. R.).

<sup>1</sup> To whom correspondence should be addressed: Dept. of Physiology, The University of Tennessee Health Science Center, 894 Union Ave., Memphis, TN 38163. Tel.: 901-448-7321; Fax: 901-448-7126; E-mail: rgadipar@uthsc.edu.

<sup>2</sup> The abbreviations used are: VEGF, vascular endothelial growth factor; EC, endothelial cell; HRMVEC, human microvascular endothelial cell; OIR, oxy-

gen-induced retinopathy; PLD1, phospholipase D1; cPLA<sub>2</sub>, cytosolic phospholipase A<sub>2</sub>; iPLA<sub>2</sub>, calcium-independent phospholipase A<sub>2</sub>; AA, arachidonic acid; PUFA, polyunsaturated fatty acid; PKC, protein kinase C; PP1, 4-amino-5-(4-methylphenyl)-7-(*t*-butyl)pyrazolo[3,4-*d*]pyrimidine; TRITC, tetramethylrhodamine isothiocyanate; P, postpartum day; dn, dominant negative.

## VEGF-induced Retinal Neovascularization Requires cPLA<sub>2</sub>

PLD1, and PKC $\gamma$  in HRMVECs. In addition, Src-PLD1-PKC $\gamma$ -dependent cPLA<sub>2</sub> activation and AA release are required for VEGF-induced HRMVEC DNA synthesis, migration, and tube formation. Interestingly enough, Src-PLD1-PKC $\gamma$ -cPLA<sub>2</sub> activation is also needed for hypoxia-induced VEGF-mediated pathological retinal neovascularization in a mouse model of OIR.

### MATERIALS AND METHODS

**Reagents**—Growth factor-reduced Matrigel was obtained from BD Biosciences. Recombinant human VEGF165 was bought from R&D Systems (Minneapolis, MN). 4-Amino-5-(4-methylphenyl)-7-(*t*-butyl)pyrazolo[3,4-*d*]pyrimidine (PP1) was purchased from EMD Chemicals (La Jolla, CA). 1-Butanol, FITC-conjugated anti-rabbit IgG, high molecular weight (~2,000,000) fluorescein-conjugated dextran, and TRITC-conjugated anti-rabbit IgG were purchased from Sigma. Anti- $\beta$ -tubulin, anti-cPLA<sub>2</sub>, anti-ERK2, anti-JNK1, anti-p38MAPK, anti-MEK1, anti-PKC $\gamma$ , and anti-VEGF antibodies were purchased from Santa Cruz Biotechnology Inc. (Santa Cruz, CA). Anti-phospho-cPLA<sub>2</sub>, anti-phospho-ERK1/2, anti-phospho-JNK, anti-phospho-p38MAPK, anti-phospho-PKC $\gamma$ , anti-phospho-PLD1, anti-phospho-Src, and anti-PLD1 antibodies were obtained from Cell Signaling Technology (Beverly, MA). Anti-Src antibodies were bought from Millipore (Temecula, CA). Anti-CD31 antibodies were purchased from BD Biosciences. Anti-phospho-cPLA<sub>2</sub> antibodies were obtained from Abcam (Cambridge, MA). cPLA<sub>2</sub> assay kit was bought from Cayman Chemicals (Ann Arbor, MI). Human scrambled siRNA (ON-TARGETplus Non-targeting Pool), human PKC $\gamma$  siRNA (ON-TARGETplus SMARTpool, L-004654-00-0010), human cPLA<sub>2</sub> siRNA (ON-TARGETplus SMARTpool L-009886-00-0010), human PLD1 siRNA (ON-TARGETplus SMARTpool L-009413-00-0010), mouse scrambled siRNA (ON-TARGETplus Non-targeting Pool D-001810-10-20), mouse PKC $\gamma$  siRNA (ON-TARGETplus SMARTpool L-050293-00-0010), mouse cPLA<sub>2</sub> siRNA (ON-TARGETplus SMARTpool L-063167-01-0020), mouse PLD1 siRNA (ON-TARGETplus SMARTpool L-040014-01-0020), mouse Src siRNA (ON-TARGETplus SMARTpool L-040877-00-0010), and mouse VEGF siRNA (ON-TARGETplus SMARTpool L-040812-00-0020) were obtained from Thermo Scientific (Chicago, IL). Vectashield HardSet mounting medium and Vectashield HardSet mounting medium with DAPI were purchased from Vector Laboratories (Burlingame, CA). Alexa Fluor 350 goat anti-rat IgG was bought from Molecular Probes (Eugene, OR). [<sup>3</sup>H]Thymidine (specific activity 20 Ci/mmol), and [<sup>3</sup>H]AA (specific activity 202 Ci/mmol) were obtained from PerkinElmer Life Sciences. The construction of Ad-GFP, Ad-dnJNK1, Ad-dnMEK1, Ad-dnp38MAPK, and Ad-dnSrc were described previously (29, 30).

**Cell Culture**—HRMVECs (catalogue No. ACBRI 181) were purchased from the Applied Cell Biology Research Institute (Kirkland, WA) and grown in Medium 131 containing microvascular growth supplements, 10  $\mu$ g/ml gentamycin, and 0.25  $\mu$ g/ml amphotericin B. Cultures were maintained at 37 °C in a humidified 95% air, 5% CO<sub>2</sub> atmosphere. HRMVECs with passage numbers between 5 and 10 were growth-arrested by incu-

bating them in Medium 131 for 12 h and used to perform the experiments unless otherwise indicated.

**AA Release**—[<sup>3</sup>H]AA release from HRMVECs prelabeled with [<sup>3</sup>H]AA (0.5  $\mu$ Ci/ml) was measured as described previously and expressed as counts/min/dish (31).

**Cell Migration**—Cell migration was measured using a modified Boyden chamber method as described previously (29), and the values are expressed as number of migrated cells/field.

**cPLA<sub>2</sub> Assay**—cPLA<sub>2</sub> activity in the retinal extracts was measured using a kit following the manufacturer's instructions (Cayman Chemicals). Briefly, 10  $\mu$ l of the retinal extracts containing an equal amount of protein was mixed with 5  $\mu$ l of 10  $\mu$ M bromoenol lactone followed by the addition of 200  $\mu$ l of 1.5 M substrate (arachidonyl thio-phosphatidylcholine) and incubation at room temperature for 60 min. Reaction was stopped by adding 10  $\mu$ l of 5,5'-dithio-bis(2-nitrobenzoic acid) (DTNB), and the absorbance was measured at 405 nm in a Spectramax 190 microplate reader (Molecular Devices, Sunnyvale CA). Assays were performed in triplicate, and cPLA<sub>2</sub> activity was calculated using the extinction coefficient value of 12.8 mM<sup>-1</sup> cm<sup>-1</sup> for 5,5'-dithio-bis(2-nitrobenzoic acid). The cPLA<sub>2</sub> activity was expressed as nanomol of substrate hydrolyzed/min/ml.

**DNA Synthesis**—DNA synthesis was measured by [<sup>3</sup>H]thymidine incorporation as described previously and expressed as counts/min/dish (32).

**Tube Formation**—Tube formation was measured as described previously (29). The tube-like structures were observed under a phase contrast light microscope (Nikon Eclipse TS100, type ADL; magnification  $\times$ 10/NA 0.25), and the images were captured by a charge-coupled device camera (KP-D20AU, Hitachi) using Apple iMovie 7.1.4 software. The tube length, calculated using NIH ImageJ version 1.43, was expressed in micrometers.

**Western Blotting**—Cell or tissue extracts containing an equal amount of protein were resolved by electrophoresis on 0.1% (w/v) SDS and 10% (w/v) polyacrylamide gels. The proteins were transferred electrophoretically to a nitrocellulose membrane. After blocking in either 5% (w/v) nonfat dry milk or 5% (w/v) BSA, the membrane was probed with the appropriate primary antibodies followed by incubation with HRP-conjugated secondary antibodies. The antigen-antibody complexes were detected using an enhanced chemiluminescence detection reagent kit (Amersham Biosciences).

**Transfections and Infections**—HRMVECs were transfected with scrambled or target gene siRNA molecules at a final concentration of 100 nM using Lipofectamine 2000 transfection reagent according to the manufacturer's instructions. When adenoviral vectors were used to deliver the dominant negative mutant of a specific gene, cells were infected with adenovirus carrying GFP or target gene at 40 multiplicities of infection overnight in complete medium. After transfections or infections, cells were growth-arrested in microvascular growth supplement-free Medium 131 for 24 h and used as required. In the case of transfections *in vivo*, siRNA molecules at 1  $\mu$ g/0.5  $\mu$ l/eye were injected intravitreally using a 33-gauge needled syringe.

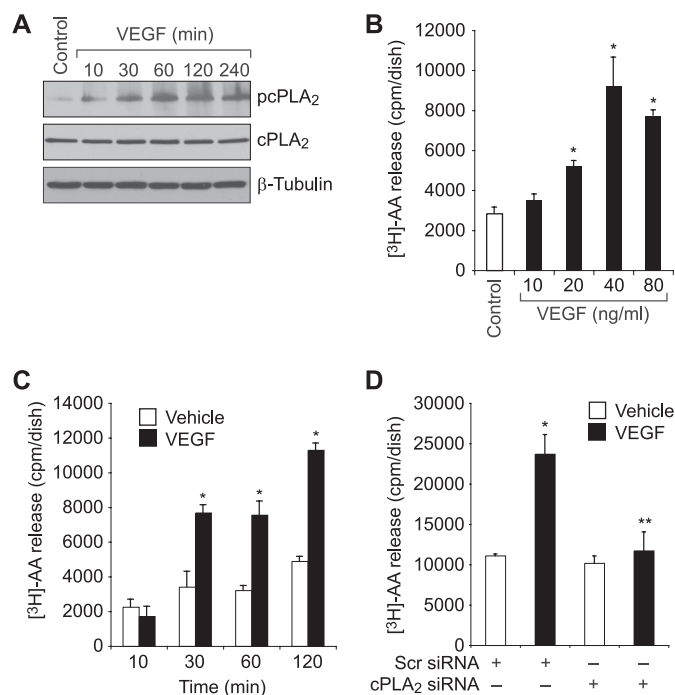


**FIGURE 1. VEGF induces AA release via activation of cPLA<sub>2</sub> in HRMVECs.** A, quiescent HRMVECs were treated with and without 40 ng/ml VEGF for the indicated time periods, and cell extracts were prepared and analyzed for cPLA<sub>2</sub> phosphorylation by Western blotting using its phosphospecific antibodies. The blot was reprobed sequentially with anti-cPLA<sub>2</sub> and anti- $\beta$ -tubulin antibodies for normalization. B, HRMVECs that were prelabeled with [<sup>3</sup>H]AA and growth-arrested were treated with and without the indicated doses of VEGF for 1 h, and [<sup>3</sup>H]AA released into the medium was measured. C, all conditions were the same as in B except that cells were treated with and without VEGF (40 ng/ml) for the indicated time periods, and [<sup>3</sup>H]AA released into the medium was measured. D, HRMVECs in which cPLA<sub>2</sub> was down-regulated by its siRNA (100 nM) were prelabeled with [<sup>3</sup>H]AA, growth-arrested, and treated with and without VEGF (40 ng/ml) for 1 h, and the [<sup>3</sup>H]AA released into the medium was measured. The bar graphs in B–D represent the quantitative analysis of three independent experiments. The values are presented as mean  $\pm$  S.D. \*,  $p < 0.01$  versus vehicle control or scrambled (Scr) siRNA; \*\*,  $p < 0.01$  versus scrambled siRNA + VEGF.

**Retinal Angiogenesis**—All experiments involving the use of animals were approved by the Animal Care and Use Committee of the University of Tennessee Health Science Center, Memphis, TN. Retinal angiogenesis was performed according to the method of Connor *et al.* (33). C57BL/6J mice pups (P7) with nursing mothers were exposed to 75% oxygen for 5 days and then returned to room air at P12. Mice pups of the same age kept at room air were used as controls. After exposure to hyperoxia, mice pups were administered scrambled siRNA, cPLA<sub>2</sub> siRNA or VEGF siRNA (1  $\mu$ g/0.5  $\mu$ l/eye) at P13, P14, and P15 by intravitreal injections using a 33-gauge needle. The mice pups were sacrificed at P17 after intracardiac perfusion with high molecular weight FITC-dextran in PBS. Eyes were enucleated and fixed in 4% (v/v) paraformaldehyde for 6 to 24 h at room temperature. Retinas were isolated, flat-mounted, placed under a coverslip, examined under a Zeiss inverted fluorescence microscope (AxioVision AX10), and quantified using Nikon NIS-Elements software version AR 3.1. Retinal vasculature was determined by calculating the ratio of fluorescence intensity to total retinal area. Retinal tufts and/or counting proliferating ECs were used to evaluate the retinal neovascularization. Neovascularization was quantified either by dividing the tufts area

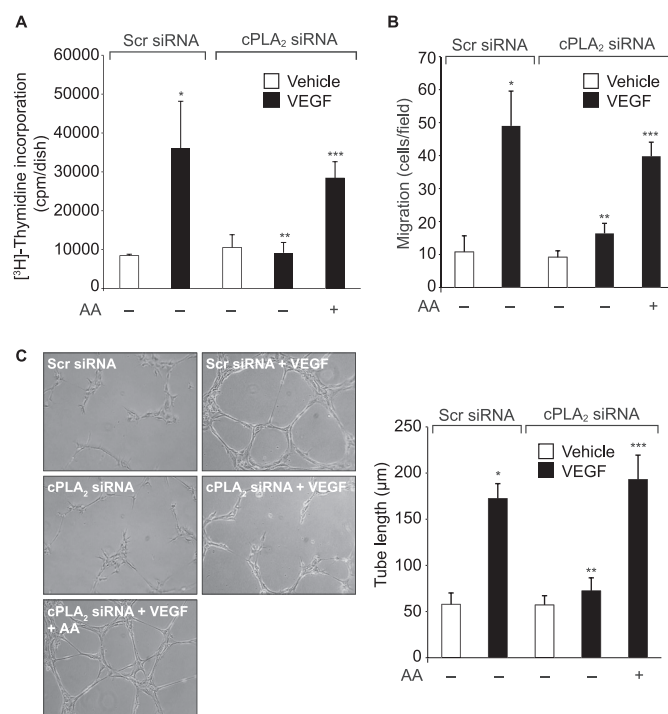


**FIGURE 2. AA rescues HRMVEC DNA synthesis, migration, and tube formation from inhibition by cPLA<sub>2</sub> down-regulation.** A–C, HRMVECs that were transfected with scrambled or cPLA<sub>2</sub> siRNA (100 nM) and growth-arrested were treated with and without VEGF (40 ng/ml) in the presence and absence of exogenously added AA (10  $\mu$ M), and DNA synthesis (A), migration (B), and tube formation (C) were measured as described under “Materials and Methods.” The bar graphs in A–C represent the quantitative analysis of three independent experiments. The values are presented as mean  $\pm$  S.D. \*,  $p < 0.01$  versus scrambled (Scr) siRNA; \*\*,  $p < 0.01$  versus scrambled siRNA + VEGF; \*\*\*,  $p < 0.01$  versus cPLA<sub>2</sub> siRNA + VEGF.

by the total retinal area or counting the CD31- and Ki67-positive cells that extended anterior to the inner limiting membrane per section ( $n = 3$  eyes, 5 sections/eye).

**Immunofluorescence Staining**—After hyperoxia, mice pups were returned to room air for 3 days, at which time they were sacrificed, eyes were enucleated and fixed in OCT compound, and cryosections were prepared. To detect the phosphorylation of cPLA<sub>2</sub> in the retina, after blocking in normal goat serum, the cryosections (5  $\mu$ m) were probed with rabbit anti-human phospho-cPLA<sub>2</sub> (Ser-505) antibodies (1:100) and rat anti-mouse CD31 antibodies (1:100) in a humidified chamber for 1 h at room temperature followed by incubation with Alexa Fluor 568-conjugated goat anti-rabbit and Alexa Fluor 488-conjugated-goat anti-rat secondary antibodies. Normal serum from rabbit and/or rat was used as a control. To identify proliferating ECs, after blocking in normal goat serum, the cryosections were probed with rabbit anti-mouse Ki67 antibodies (1:100) and rat anti-mouse CD31 antibodies (1:100) followed by incubation with TRITC-conjugated goat anti-rabbit and FITC-conjugated goat anti-rat secondary antibodies. The sections were observed under a Zeiss inverted microscope (Zeiss AxioVision AX10; type LD plan-Neofluar, magnification  $\times 40$ /NA 0.6; or type plan-Apochromat, magnification  $\times 10$ /NA 0.45), and the fluorescence images were captured by a Zeiss AxioCam MRm camera using the microscope-operating and image analysis software AxioVision 4.7.2 (Carl Zeiss Imaging Solutions GmbH).

## VEGF-induced Retinal Neovascularization Requires cPLA<sub>2</sub>

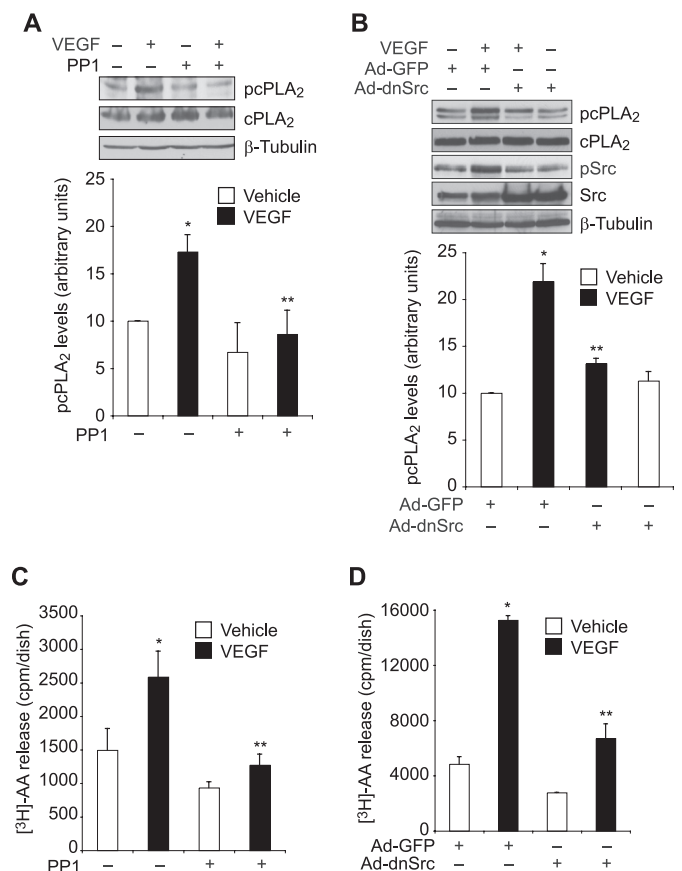


**FIGURE 3. Src mediates VEGF-induced cPLA<sub>2</sub> phosphorylation and AA release in HRMVECs.** *A*, quiescent HRMVECs were treated with and without VEGF (40 ng/ml) in the presence or absence of PP1 (10  $\mu$ M) for 30 min, and cell extracts were prepared and analyzed by Western blotting for cPLA<sub>2</sub> phosphorylation using its phosphospecific antibodies. The blot was reprobbed sequentially with anti-cPLA<sub>2</sub> and anti- $\beta$ -tubulin antibodies for normalization. *B*, all conditions were the same as in *A* except that cells were transfected with Ad-GFP or Ad-dnSrc at 40 multiplicities of infection and growth-arrested before subjecting them to treatment with and without VEGF (40 ng/ml) for 30 min and analyzing the cell extracts for cPLA<sub>2</sub> and Src phosphorylation. The blot was reprobbed sequentially with anti-cPLA<sub>2</sub>, anti-Src, and anti- $\beta$ -tubulin antibodies for normalization or to show overexpression of dominant negative Src. *C*, HRMVECs that were prelabeled with [<sup>3</sup>H]AA and growth-arrested were treated with and without VEGF (40 ng/ml) in the presence and absence of PP1 (10  $\mu$ M) for 1 h, and [<sup>3</sup>H]AA released into the medium was measured. *D*, all conditions were the same as in *B* except that cells were transfected with Ad-GFP or Ad-dnSrc at 40 multiplicities of infection and prelabeled with [<sup>3</sup>H]AA before subjecting them to treatment with and without VEGF (40 ng/ml) for 1 h and measuring [<sup>3</sup>H]AA released into the medium. The values are presented as mean  $\pm$  S.D. \*,  $p < 0.01$  versus vehicle control or Ad-GFP control; \*\*,  $p < 0.01$  versus VEGF or Ad-GFP + VEGF.

**Statistics**—All of the experiments were repeated three times, and data are presented as mean  $\pm$  S.D. The treatment effects were analyzed by Student's *t* test, and *p* values  $< 0.05$  were considered statistically significant. In the case of Western blot analysis, immunofluorescence staining, and retinal angiogenesis, one set of data is presented.

## RESULTS

**VEGF-induced HRMVEC DNA Synthesis, Migration, and Tube Formation Require cPLA<sub>2</sub>-mediated AA Release**—Recent studies have suggested that PUFA such as AA play a role in the regulation of angiogenesis (27, 28). Because cPLA<sub>2</sub> hydrolyzes glycerophospholipids with AA at the sn-2 position, we hypothesized that cPLA<sub>2</sub>-dependent AA release is required for patho-

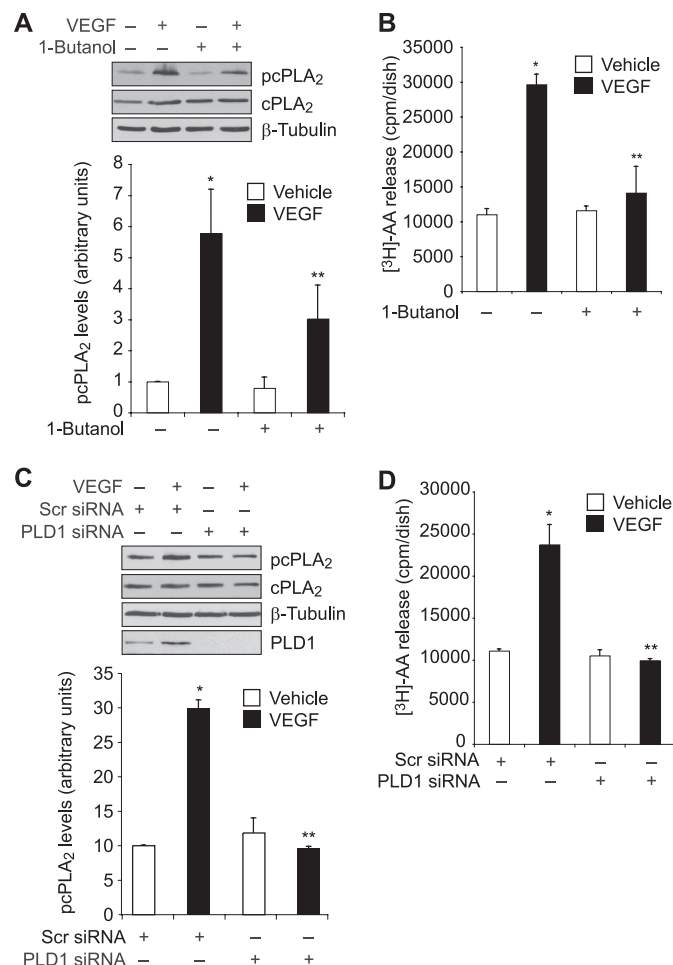


**FIGURE 4. PLD1 mediates VEGF-induced cPLA<sub>2</sub> phosphorylation and AA release in HRMVECs.** *A*, quiescent HRMVECs were treated with and without VEGF (40 ng/ml) in the presence or absence of 1-butanol (0.25% v/v) for 30 min, and cell extracts were prepared and analyzed by Western blotting for cPLA<sub>2</sub> phosphorylation using its phosphospecific antibodies. The blot was reprobbed sequentially with anti-cPLA<sub>2</sub> and anti- $\beta$ -tubulin antibodies for normalization. *B*, HRMVECs that were prelabeled with [<sup>3</sup>H]AA and growth-arrested were treated with and without VEGF (40 ng/ml) in the presence and absence of 1-butanol (0.25% v/v) for 1 h, and [<sup>3</sup>H]AA released into the medium was measured. *C*, all conditions were the same as in *A* except that cells were transfected with scrambled (Scr) or PLD1 siRNA and growth-arrested before subjecting them to treatment with and without VEGF (40 ng/ml) for 30 min and analyzing them for cPLA<sub>2</sub> phosphorylation. The blot was reprobbed sequentially with anti-cPLA<sub>2</sub>, anti- $\beta$ -tubulin, and anti-PLD1 antibodies for normalization or to show the down-regulation of PLD1 by its siRNA. *D*, all conditions were the same as in *B* except that cells were transfected with scrambled (Scr) or PLD1 siRNA and prelabeled with [<sup>3</sup>H]AA before subjecting them to treatment with and without VEGF (40 ng/ml) for 1 h and measuring [<sup>3</sup>H]AA released into the medium. The bar graphs in *A–D* represent the quantitative analysis of three independent experiments. The values are presented as mean  $\pm$  S.D. \*,  $p < 0.01$  versus vehicle control or scrambled siRNA; \*\*,  $p < 0.01$  versus VEGF or scrambled siRNA + VEGF.

logical retinal angiogenesis. To address this hypothesis, we tested the effect of VEGF on cPLA<sub>2</sub> activation and AA release in HRMVECs. VEGF stimulated cPLA<sub>2</sub> phosphorylation in a time-dependent manner in HRMVECs (Fig. 1*A*). VEGF also induced AA release in a dose- and time-dependent manner in HRMVECs (Fig. 1, *B* and *C*). In addition, siRNA-mediated depletion of cPLA<sub>2</sub> levels abolished VEGF-induced AA release (Fig. 1*D*). Similarly, siRNA-mediated depletion of cPLA<sub>2</sub> levels inhibited VEGF-induced HRMVEC DNA synthesis, migration, and tube formation (Fig. 2, *A*, *B*, and *C*). If activation of cPLA<sub>2</sub> is

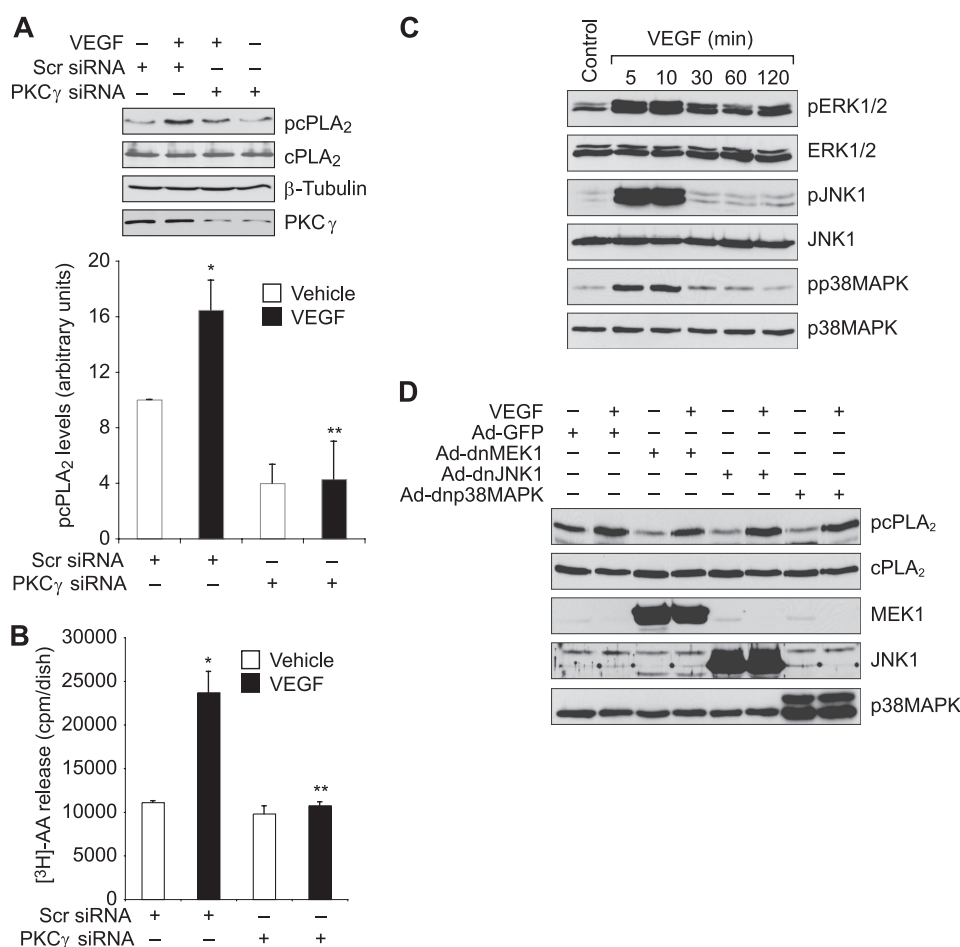


**FIGURE 5. PKC $\gamma$  mediates VEGF-induced cPLA<sub>2</sub> phosphorylation and AA release in HRMVECs.** *A*, HRMVECs were transfected with scrambled (*Scr*) or PKC $\gamma$  siRNA, made quiescent, and treated with and without VEGF (40 ng/ml) for 30 min; cell extracts were prepared and analyzed by Western blotting for cPLA<sub>2</sub> phosphorylation using its phosphospecific antibodies. The blot was reprobbed sequentially with anti-cPLA<sub>2</sub>, anti- $\beta$ -tubulin, and anti-PKC $\gamma$  antibodies for normalization or to show the down-regulation of PKC $\gamma$  by its siRNA. *B*, HRMVECs were transfected with scrambled or PKC $\gamma$  siRNA, prelabeled with [<sup>3</sup>H]AA, growth-arrested, and treated with and without VEGF (40 ng/ml) for 1 h, and [<sup>3</sup>H]AA released into the medium was measured. *C*, quiescent HRMVECs were treated with and without VEGF (40 ng/ml) for the indicated time periods, and cell extracts were prepared and analyzed by Western blotting for ERK1/2, JNK1, and p38MAPK phosphorylation using their phosphospecific antibodies. The blots were reprobbed with anti-ERK2, anti-JNK1, or anti-p38MAPK antibodies for normalization. *D*, HRMVECs that were infected with Ad-dnMEK1, Ad-dnJNK1, or Ad-dnp38MAPK and growth-arrested were treated with and without VEGF (40 ng/ml) for 30 min, and cell extracts were prepared. Cell extracts containing an equal amount of protein from control and each treatment were analyzed by Western blotting for cPLA<sub>2</sub> phosphorylation using its phosphospecific antibodies. The blot was reprobbed sequentially with anti-cPLA<sub>2</sub>, anti-MEK1, anti-JNK1, and anti-p38MAPK antibodies for normalization or to show the overexpression of dnMEK1, dnJNK1, or dnp38MAPK. The bar graphs in *A* and *B* represent quantitative analyses of three independent experiments. The values are presented as mean  $\pm$  S.D. \* $p$  < 0.01 versus scrambled (*Scr*) siRNA; \*\* $p$  < 0.01 versus scrambled siRNA + VEGF.

sufficient to mediate VEGF-induced HRMVEC angiogenic responses, then exogenous addition of AA should be able to rescue VEGF-induced HRMVEC DNA synthesis, migration, and tube formation from inhibition by cPLA<sub>2</sub> depletion. Indeed, the exogenous addition of AA rescued VEGF-induced HRMVEC DNA synthesis, migration, and tube formation from inhibition by siRNA-mediated cPLA<sub>2</sub> down-regulation (Fig. 2, *A*, *B*, and *C*).

**Src Mediates VEGF-induced cPLA<sub>2</sub> Activation and AA Release**—Src plays an essential role in VEGF-induced angiogenesis (7, 34). To find a link between Src and cPLA<sub>2</sub>, we studied the role of Src in VEGF-induced cPLA<sub>2</sub> phosphorylation. PP1, a potent and specific inhibitor of Src (35) attenuated VEGF-induced cPLA<sub>2</sub> phosphorylation (Fig. 3*A*). To confirm this observation, we blocked Src activation via adenovirus-mediated expression of its dominant negative mutant (dnSrc) and tested its effect on VEGF-induced cPLA<sub>2</sub> phosphorylation. Adenovirus-mediated expression of dnSrc diminished VEGF-

induced cPLA<sub>2</sub> phosphorylation (Fig. 3*B*). Both PP1 and dnSrc blocked VEGF-induced AA release (Fig. 3, *C* and *D*). These observations indicate that Src mediates VEGF-induced cPLA<sub>2</sub> phosphorylation and AA release.

**PLD1 Mediates VEGF-induced cPLA<sub>2</sub> Activation and AA Release**—As we had previously shown that Src mediates VEGF-induced PLD1 activation (19), next we wanted to find whether PLD1 plays a role in VEGF-induced cPLA<sub>2</sub> phosphorylation. 1-Butanol, a potent and specific inhibitor of PLD1 (36), attenuated VEGF-induced cPLA<sub>2</sub> phosphorylation (Fig. 4*A*). In addition, siRNA-mediated down-regulation of PLD1 levels blocked VEGF-induced cPLA<sub>2</sub> phosphorylation (Fig. 4*C*). Consistent with these observations, either PLD1 inhibition by 1-butanol or its down-regulation by siRNA diminished VEGF-induced AA release (Fig. 4, *B* and *D*). Together, these results suggest that PLD1 is required for VEGF-induced cPLA<sub>2</sub> phosphorylation and AA release.

## VEGF-induced Retinal Neovascularization Requires cPLA<sub>2</sub>

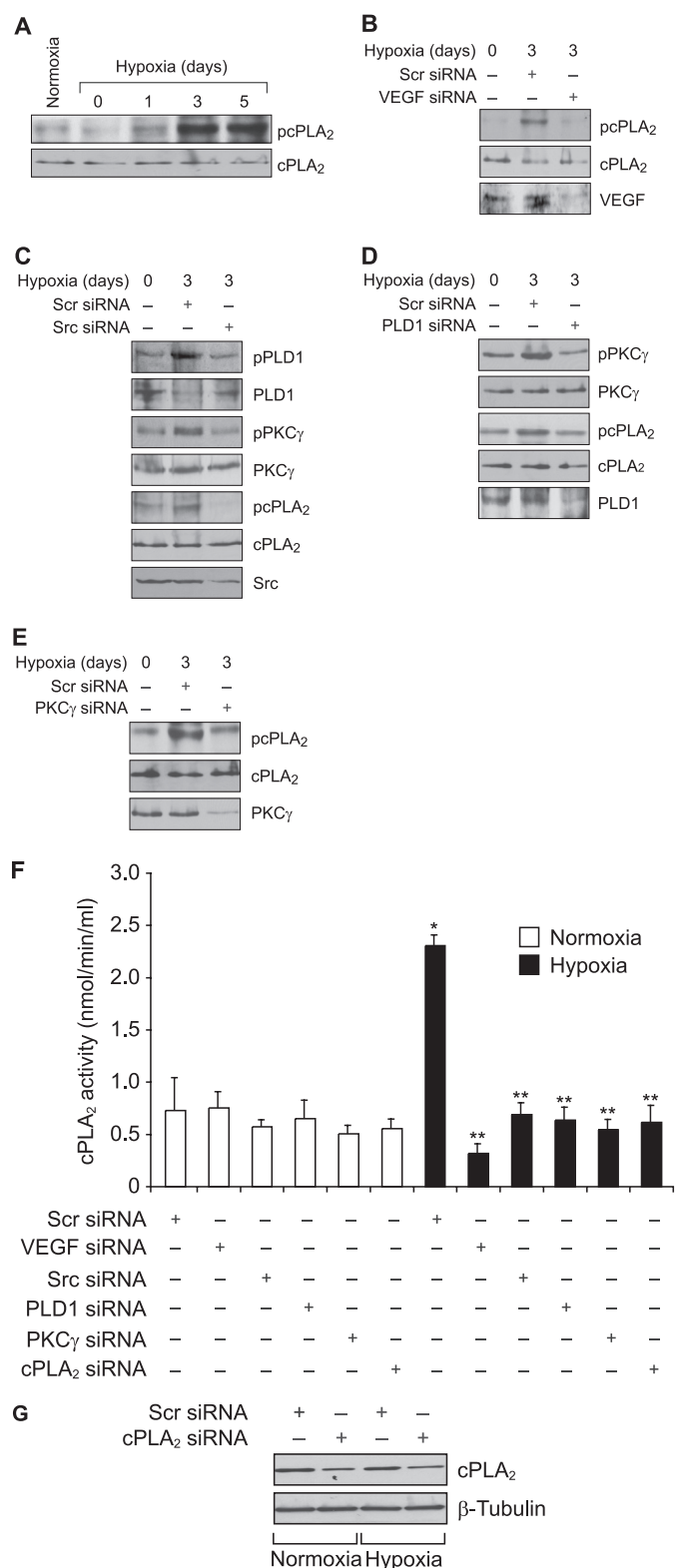


**FIGURE 6. Hypoxia stimulates cPLA<sub>2</sub> phosphorylation via Src-PLD1-PKCγ signaling axis in retina.** A, C57BL/6 mice pups were exposed to 75% oxygen from P7 to P12 at which time they were returned to normoxia to develop relative hypoxia for the indicated time periods; eyes were enucleated, retinas were isolated, and tissue extracts were prepared and analyzed by Western blotting for cPLA<sub>2</sub> phosphorylation using its phosphospecific antibodies. The blot was reprobbed with anti-cPLA<sub>2</sub> antibodies for normalization. B, after exposure to hyperoxia, mice pups were returned to normoxia and administered 1 μg/0.5 μl scrambled (Scr) or VEGF siRNA at P12 and P13 by intravitreal injections. Retinas were isolated at P15, and extracts were prepared and analyzed

*PKCγ Mediates VEGF-induced cPLA<sub>2</sub> Activation and AA Release*—The PKC family of serine/threonine kinases includes several members that are classified as conventional ( $\alpha$ ,  $\beta$ , and  $\gamma$ ), novel ( $\delta$ ,  $\epsilon$ ,  $\eta$  and  $\theta$ ), or atypical ( $\zeta$ ,  $\iota$ , and  $\mu$ ) (37). Previously, we had reported that VEGF stimulates PKC $\gamma$  downstream of Src-PLD1 in HRMVECs (19). Therefore, we wanted to find whether PKC $\gamma$  also plays a role in VEGF-induced cPLA<sub>2</sub> phosphorylation and AA release. To test this assumption, PKC $\gamma$  was down-regulated using its siRNA and tested for its effect on VEGF-induced cPLA<sub>2</sub> phosphorylation and AA release. Down-regulation of PKC $\gamma$  levels by its siRNA attenuated VEGF-induced cPLA<sub>2</sub> phosphorylation and AA release (Fig. 5, A and B). Together, these observations show that VEGF-induced cPLA<sub>2</sub> phosphorylation and AA release require activation of Src-PLD1-PKC $\gamma$  signaling. Previous studies had demonstrated that MAPKs play a role in agonist-induced cPLA<sub>2</sub> activation (38, 39). Therefore, to find whether MAPKs play a role in VEGF-induced cPLA<sub>2</sub> activation, we also studied the role of ERK1/2, JNK1, and p38MAPK. VEGF induced phosphorylation of ERK1/2, JNK1, and p38MAPK in a time-dependent manner in HRMVECs (Fig. 5C). However, a blockade of ERK1/2, JNK1, and p38MAPK by adenovirus-mediated expression of dnMEK1 (dnMEK1 blocks ERK1/2 phosphorylation), dnJNK1, and dnp38MAPK, respectively, had no significant effect on VEGF-induced cPLA<sub>2</sub> phosphorylation (Fig. 5D).

*Hypoxia Induces cPLA<sub>2</sub> Phosphorylation via VEGF-Src-PLD1-PKCγ Signaling*—The above findings clearly indicated a role for cPLA<sub>2</sub>-mediated AA release in VEGF-induced HRMVEC DNA synthesis, migration, and tube formation. To validate these *in vitro* observations *in vivo*, we used a mouse model of OIR. After exposure to hyperoxia from P7 to P12, the mice pups were returned to normoxia to create a relative hypoxia. At various time periods of hypoxia, retinal extracts were prepared

by Western blotting for cPLA<sub>2</sub> phosphorylation using its phosphospecific antibodies. The blot was reprobbed sequentially with anti-cPLA<sub>2</sub> and anti-VEGF antibodies for normalization or to show down-regulation of VEGF by its siRNA. C, all conditions were the same as in B except that mice pups were administered scrambled or Src siRNA at P12 and P13 by intravitreal injections, and at P15 the retinas were isolated, and extracts were prepared and analyzed for phosphorylation of PLD1, PKC $\gamma$ , and cPLA<sub>2</sub> using their phosphospecific antibodies. The blots were reprobbed with anti-PLD1, anti-PKC $\gamma$ , anti-cPLA<sub>2</sub>, or anti-Src antibodies either for normalization or to show the down-regulation of Src by its siRNA. D, all conditions were the same as in B except that mice pups were administered scrambled or PLD1 siRNA at P12 and P13 by intravitreal injections, and at P15 the retinas were isolated and extracts prepared and analyzed for phosphorylation of PKC $\gamma$  and cPLA<sub>2</sub> using their phosphospecific antibodies. The blots were reprobbed with anti-PKC $\gamma$ , anti-cPLA<sub>2</sub>, or anti-PLD1 antibodies either for normalization or to show the down-regulation of PLD1 by its siRNA. E, all conditions were the same as in B except that mice pups were administered scrambled or PKC $\gamma$  siRNA at P12 and P13 by intravitreal injections, and at P15 the retinas were isolated and extracts prepared and analyzed for phosphorylation of cPLA<sub>2</sub> using its phosphospecific antibodies. The blot was reprobbed sequentially with anti-cPLA<sub>2</sub> and anti-PKC $\gamma$  antibodies either for normalization or to show the down-regulation of PKC $\gamma$  by its siRNA. F, after exposure to hyperoxia, mice pups were returned to normoxia and administered 1 μg/0.5 μl scrambled, VEGF, Src, PLD1, PKC $\gamma$ , or cPLA<sub>2</sub> siRNA at P12 and P13 by intravitreal injections. Retinas were isolated at P15, and extracts were prepared and analyzed for cPLA<sub>2</sub> activity. G, retinal extracts of scrambled or cPLA<sub>2</sub> siRNA-injected mice pup eyes were analyzed by Western blotting for cPLA<sub>2</sub> levels using its specific antibodies, and the blot was reprobbed with anti- $\beta$ -tubulin antibodies for normalization. The results were reproduced in three different experiments and presented as mean  $\pm$  S.D. \*,  $p < 0.01$  versus scrambled siRNA + normoxia; \*\*,  $p < 0.01$  versus scrambled siRNA + hypoxia.

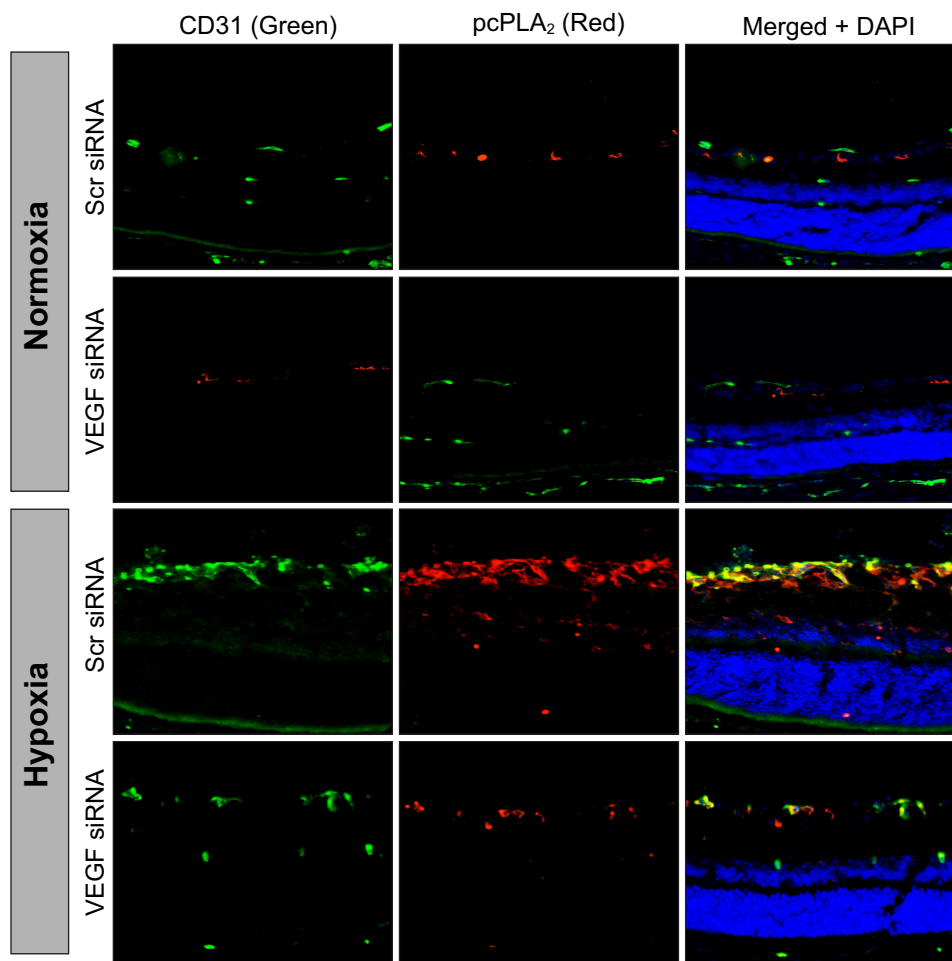


FIGURE 7. **Depletion of VEGF inhibits hypoxia-induced cPLA<sub>2</sub> phosphorylation in retinal ECs.** After exposure to 75% oxygen from P7 to P12, mice pups were returned to normoxia and administered 1  $\mu\text{g}/0.5 \mu\text{l}$  scrambled (Scr) or VEGF siRNA at P12 and P13 by intravitreal injections. At P15, mice pups were sacrificed, eyes were enucleated and fixed, and cross-sections were prepared and analyzed by double immunofluorescence staining for pcPLA<sub>2</sub> along with CD31 as described under "Materials and Methods."

and analyzed for cPLA<sub>2</sub> phosphorylation. Subjecting mice pups to hypoxia caused an increase in the phosphorylation of cPLA<sub>2</sub> with the maximum effect at day 3 (Fig. 6A). To find whether hypoxia-induced cPLA<sub>2</sub> phosphorylation requires VEGF, VEGF levels were down-regulated by injecting its siRNA into the vitreous humor at P12 and P13, and cPLA<sub>2</sub> phosphorylation in the retina was measured at day 3 (P15) of hypoxia. VEGF down-regulation significantly attenuated hypoxia-induced cPLA<sub>2</sub> phosphorylation (Fig. 6B). Because the *in vitro* observations showed that VEGF-induced cPLA<sub>2</sub> phosphorylation requires activation of Src-PLD1-PKC $\gamma$ , we next tested the role of this signaling axis in hypoxia-induced cPLA<sub>2</sub> phosphorylation. Depletion of Src, PLD1, and PKC $\gamma$  levels by their respective siRNAs attenuated hypoxia-induced cPLA<sub>2</sub> phosphorylation (Fig. 6, C–E). In addition, whereas down-regulation of Src levels attenuated both PLD1 and PKC $\gamma$  phosphorylation (Fig. 6C), depletion of PLD1 levels blocked only PKC $\gamma$  phosphorylation (Fig. 6D). Consistent with the role of VEGF-Src-PLD1-PKC $\gamma$  signaling in hypoxia-induced cPLA<sub>2</sub> phosphorylation, siRNA-mediated depletion of these molecules also decreased cPLA<sub>2</sub> activity (Fig. 6F). As expected, down-regulation of cPLA<sub>2</sub> levels by its siRNA attenuated hypoxia-induced cPLA<sub>2</sub> activity as well (Fig. 6, F and G). Thus, these results indicate that

hypoxia-induced cPLA<sub>2</sub> activation requires VEGF-Src-PLD1-PKC $\gamma$  signaling. To find the cell type in which hypoxia-induced cPLA<sub>2</sub> phosphorylation occurs, mice pups at day 3 of hypoxia were sacrificed and enucleated, retinas were isolated and fixed, and sections were prepared and subjected to double immunofluorescence staining for CD31 and phospho-cPLA<sub>2</sub>. Substantial increases in the phosphorylation of cPLA<sub>2</sub> were observed mostly in the ECs of the retinal ganglion cell layer under hypoxia as compared with normoxia. Down-regulation of VEGF levels via intravitreal injection of its siRNA resulted in the inhibition of hypoxia-induced cPLA<sub>2</sub> phosphorylation in ECs (Fig. 7). In addition, hypoxia increased immunostaining for CD31, suggesting enhanced proliferation of ECs.

**Oxygen-induced Retinal Neovascularization Requires cPLA<sub>2</sub> Activation**—To understand the functional significance of cPLA<sub>2</sub> in retina under hypoxic condition, its levels were depleted by intravitreal injection of its siRNA at P12 and P13, and neovascularization was measured in mice pups subjected to hypoxia or left at normoxia using retinal flat mounts. The depletion of cPLA<sub>2</sub> levels dramatically reduced hypoxia-induced retinal neovascularization as measured by decreased tufts, dilatation, or tortuosity of radial vessels (Fig. 8A). The ratio of fluorescence intensity to the total retinal area was also

## VEGF-induced Retinal Neovascularization Requires cPLA<sub>2</sub>

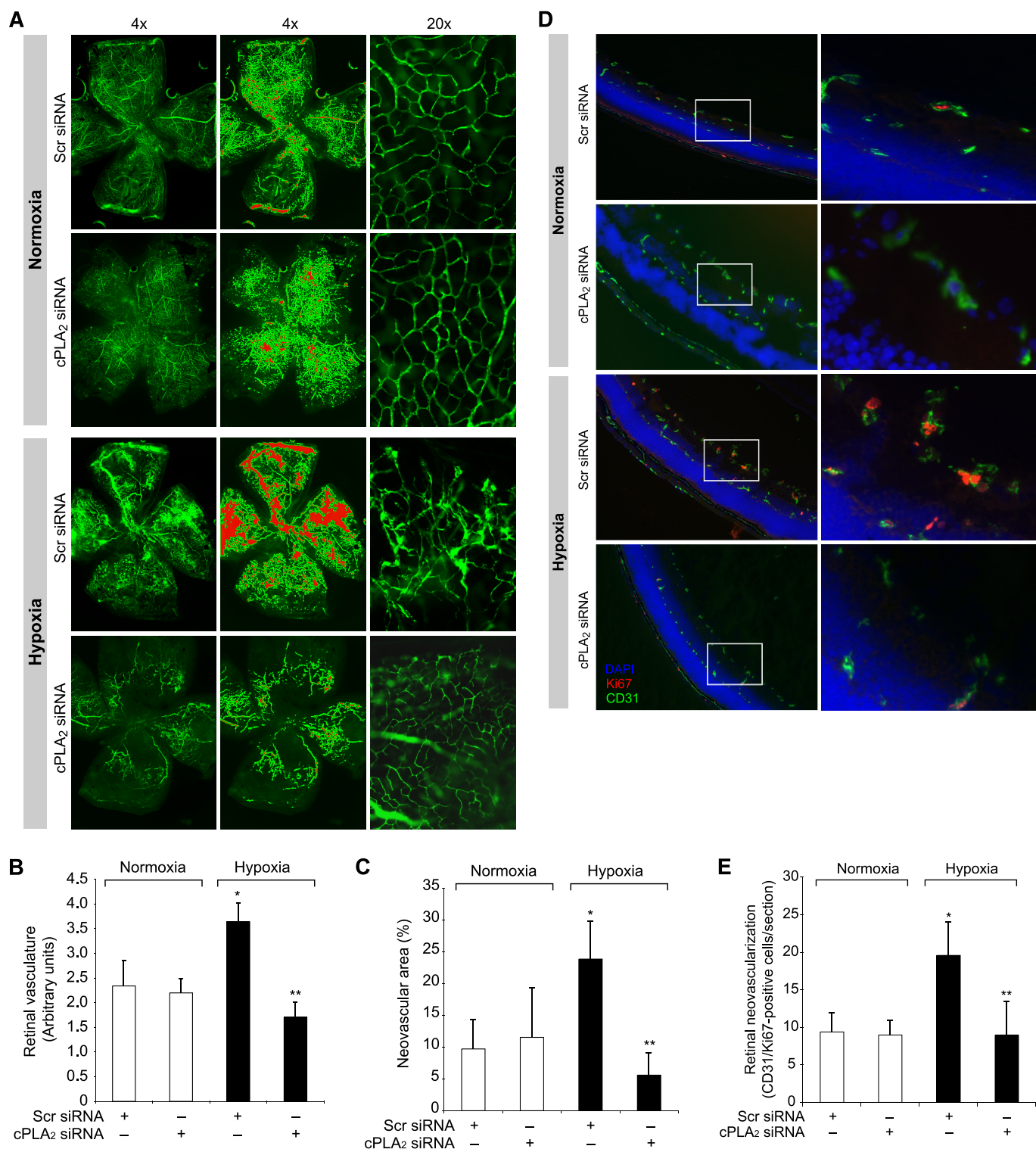


**FIGURE 8. Down-regulation of cPLA<sub>2</sub> levels blocks hypoxia-induced retinal neovascularization.** *A*, after exposure to 75% oxygen, the mice pups were returned to normoxia and administered 1  $\mu$ g/0.5  $\mu$ l scrambled (Scr) or cPLA<sub>2</sub> siRNA at P13, P14, and P15 by intravitreal injections. At P17 the pups were anesthetized, perfused with FITC-dextran, sacrificed, and enucleated; retinas were isolated, and flat mounts of whole retinas were examined for retinal neovascularization (*first column*). Neovascular tufts are highlighted with a red color (*second column*). The *third column* shows the magnified sections of selected areas of the images shown in the *first column*. *B* and *C*, retinal vasculature was measured by fluorescence intensity in the total retinal area (*B*), and the neovascular area was calculated by the percentage of tufts area to total retinal area (*C*). *D*, all conditions are the same as in *A* except that cPLA<sub>2</sub> siRNA was injected at P12 and P13, retinas were isolated at P15 and fixed, and cross-sections were made and analyzed by double immunofluorescence staining for Ki67 and CD31. The *right column* shows the higher magnification ( $\times 40$ ) of the selected areas (enclosed in rectangles) of the images shown in the *left column*. *E*, retinal neovascularization was quantified by counting Ki67- and CD31-positive cells that extended anterior to the inner limiting membrane per section ( $n = 3$  eyes, 5 sections/eye). The values are presented as mean  $\pm$  S.D. \*,  $p < 0.01$  versus normoxia + scrambled (Scr) siRNA; \*\*,  $p < 0.01$  versus hypoxia + scrambled siRNA.



decreased from  $3.64 \pm 0.38$  in the scrambled siRNA-treated group to  $1.74 \pm 0.29$  in the cPLA<sub>2</sub> siRNA-treated group (Fig. 8B). Furthermore, decreased pathological neovascularization was observed in the cPLA<sub>2</sub> down-regulated group ( $5.59 \pm 3.47\%$ ) compared with the scrambled siRNA group ( $23.84 \pm 5.86\%$ ) (Fig. 8C). To confirm the role of cPLA<sub>2</sub> in retinal neovascularization, we also measured retinal EC proliferation in mice pups subjected to hypoxia or left at normoxia. As measured by Ki67/CD31 double immunofluorescence staining, substantial increases in the number of proliferating ECs were observed in the innermost layer of the retina of hypoxia-exposed mice pups as compared with those left at normoxia (Fig. 8, D and E). The down-regulation of cPLA<sub>2</sub> levels significantly inhibited hypoxia-induced retinal EC proliferation ( $8 \pm 3.8$  Ki67-positive nuclei) compared with the scrambled siRNA group ( $17.8 \pm 3.0$  Ki67-positive nuclei) (Fig. 8, D and E).

## DISCUSSION

VEGF is a potent vascular permeability and angiogenic factor, and it plays a prominent role during development as well as in the pathogenesis of various diseases, including cancer and diabetic retinopathy (4, 5, 40–42). Intraocular VEGF levels have been found to be elevated in patients with macular degeneration and retinopathies (3). In fact, many prevailing treatments for retinal neovascularization are based on the inhibition of VEGF function (43, 44). Between the two VEGF receptors, Fms-related tyrosine kinase-1 (Flt-1) and kinase insert domain receptor/fetal liver kinase-1 (KDR/Flk-1), Flk-1 (VEGFR-2) was found to be the major mediator of VEGF actions during both embryonic and pathological angiogenesis (11, 13, 14). In regard to the role of Flt-1 (VEGFR-1) in mediating VEGF signaling events, although there is considerable lack of evidence for its role in developmental angiogenesis, many reports show that it either antagonizes VEGFR-2 or mediates only the pathological angiogenesis (12, 14). In regard to the downstream signaling events, both of the VEGFRs, upon ligand binding, lead to the activation of PLC $\gamma$  and PKC (14, 15). In addition, VEGFR-2 has been shown to stimulate PI3K-Akt-mTOR-dependent S6K1 in mediating VEGF effects in ECs (16–18).

In understanding the mechanisms of retinal neovascularization, we recently reported that activation of PLD1-PKC $\gamma$  signaling downstream of Src is essential for VEGF-induced pathological retinal angiogenesis (19). In the present study, we observed that Src-PLD1-PKC $\gamma$  signaling is required for VEGF-induced cPLA<sub>2</sub> phosphorylation and AA release in HRMVECs. Furthermore, cPLA<sub>2</sub> activation appears to be essential in mediating VEGF-induced HRMVEC angiogenic events, as its depletion negated these effects. Additional support for the role of cPLA<sub>2</sub> in VEGF-induced angiogenic responses comes from the observations that the exogenous addition of AA was found to be sufficient to rescue VEGF-induced HRMVEC DNA synthesis, migration, and tube formation from inhibition by cPLA<sub>2</sub> depletion. In addition, other studies have reported that inhibition of either cPLA<sub>2</sub> or iPLA<sub>2</sub> prevents VEGF-induced EC proliferation, supporting a role for these PLA<sub>2</sub> in the modulation of angiogenesis (24, 25). Moreover, the observations that whereas feeding mice a  $\omega$ -3 PUFA-rich diet reduces angiogenesis, a  $\omega$ -6

PUFA-rich diet enhances angiogenesis reinforce a role for PLA<sub>2</sub> in the regulation of angiogenesis (27, 28).

The novelty of the present study, however, also relates to the delineation of the mechanism of cPLA<sub>2</sub> activation by VEGF and the demonstration of the ability of its product, AA, in the mediation of not only HRMVEC growth but also the migration and tube formation of these cells. It should be noted that various studies including our own demonstrate a role for the cyclooxygenase, lipoxygenase, and cytochrome P450 monooxygenase metabolites of AA in the regulation of retinal angiogenesis (45–48). In view of these findings, it may be speculated that AA metabolism via the cyclooxygenase, lipoxygenase, and cytochrome P450 monooxygenase pathways are necessary in the mediation of various aspects of EC angiogenic responses such as proliferation, migration, and tube formation. A large number of studies have shown that both PKCs and MAPKs play a role in agonist-induced cPLA<sub>2</sub> activation (38, 39). Our observations reveal that VEGF-induced cPLA<sub>2</sub> phosphorylation requires Src-PLD1-dependent PKC $\gamma$  activation but not MAPK activation. In addition, a recent study has demonstrated that hypoxia stimulates phosphorylation of both cPLA<sub>2</sub> and p38MAPK in Müller cells of rat retina (49). However, this study also did not show any link between hypoxia-induced p38MAPK activation and cPLA<sub>2</sub> phosphorylation. In view of these observations, it is conceivable that VEGF or hypoxia-induced cPLA<sub>2</sub> phosphorylation may not require MAPK activation. Nonetheless, studies from our laboratories as well as others have shown a role for MAPKs such as JNK1 in the regulation of retinal angiogenesis (50, 51). Based on these observations, it is probable that although both cPLA<sub>2</sub> and MAPKs are required for VEGF or hypoxia-induced retinal angiogenesis, they appear to be acting independently of each other in response to these agonists/conditions.

The ability of Src-PLD1-PKC $\gamma$  signaling in the mediation of VEGF-induced cPLA<sub>2</sub> phosphorylation and AA release in HRMVECs *in vitro* also appears to be integral in hypoxia-induced retinal neovascularization in a mouse model of OIR. Consistent with our previous observations (19), hypoxia induced Src, PLD1, and PKC $\gamma$  phosphorylation in the retina. Hypoxia also induced cPLA<sub>2</sub> phosphorylation with a time course similar to that of Src, PLD1, and PKC $\gamma$  activation. In addition, in agreement with our previous observations on the cell type in which phosphorylation of Src, PLD1, and PKC $\gamma$  occurs (19), hypoxia-induced cPLA<sub>2</sub> phosphorylation was also confined mostly to ECs. Furthermore, the observation that down-regulation of Src, PLD1, and PKC $\gamma$  levels significantly suppresses the phosphorylation of their respective downstream molecules in Src-PLD1-PKC $\gamma$  signaling, in this sequential order, affecting cPLA<sub>2</sub> phosphorylation, strongly suggests that hypoxia activates this signaling axis in a contiguous manner in the retina *in vivo* as well. In addition, as depletion of VEGF levels blocked hypoxia-induced phosphorylation of Src, PLD1, PKC $\gamma$ , and cPLA<sub>2</sub>, it is conceivable that VEGF acts upstream of the activation of these signaling molecules.

As expected, the OIR-induced regression in vessel density resulted in abnormal growth of new blood vessels characterized by the presence of anastomose-like structures, bulging, and dilatation with leakiness during the hypoxia period. The finding

that hypoxia induces EC proliferation in the sprouting blood vessels and cPLA<sub>2</sub> down-regulation completely negates this effect also corroborates a role for cPLA<sub>2</sub> in retinal neovascularization. Thus, the present study provides convincing evidence for the involvement of cPLA<sub>2</sub> downstream of Src-PLD1-PKC $\gamma$  signaling in hypoxia-induced VEGF-mediated pathological retinal neovascularization.

### REFERENCES

- Gariano, R. F., and Gardner, T. W. (2005) *Nature* **438**, 960–966
- Friedlander, M. (2007) *J. Clin. Invest.* **117**, 576–586
- Aiello, L. P., Avery, R. L., Arrigg, P. G., Keyt, B. A., Jampel, H. D., Shah, S. T., Pasquale, L. R., Thieme, H., Iwamoto, M. A., Park, J. E., et al. (1994) *N. Engl. J. Med.* **331**, 1480–1487
- Pierce, E. A., Avery, R. L., Foley, E. D., Aiello, L. P., and Smith, L. E. (1995) *Proc. Natl. Acad. Sci. U.S.A.* **92**, 905–909
- Alon, T., Hemo, I., Itin, A., Pe'er, J., Stone, J., and Keshet, E. (1995) *Nat. Med.* **1**, 1024–1028
- Wang, S., Li, X., Parra, M., Verdin, E., Bassel-Duby, R., and Olson, E. N. (2008) *Proc. Natl. Acad. Sci. U.S.A.* **105**, 7738–7743
- Eliceiri, B. P., Paul, R., Schwartzberg, P. L., Hood, J. D., Leng, J., and Cheresch, D. A. (1999) *Mol. Cell* **4**, 915–924
- Gavard, J., and Gutkind, J. S. (2006) *Nat. Cell Biol.* **8**, 1223–1234
- de Vries, C., Escobedo, J. A., Ueno, H., Houck, K., Ferrara, N., and Williams, L. T. (1992) *Science* **255**, 989–991
- Terman, B. I., Dougher-Vermazen, M., Carrion, M. E., Dimitrov, D., Armellino, D. C., Gospodarowicz, D., and Böhlen, P. (1992) *Biochem. Biophys. Res. Commun.* **187**, 1579–1586
- Gille, H., Kowalski, J., Li, B., LeCouter, J., Moffat, B., Zioncheck, T. F., Pelletier, N., and Ferrara, N. (2001) *J. Biol. Chem.* **276**, 3222–3230
- Cao, R., Xue, Y., Hedlund, E. M., Zhong, Z., Tritsaris, K., Tondelli, B., Lucchini, F., Zhu, Z., Dissing, S., and Cao, Y. (2010) *Proc. Natl. Acad. Sci. U.S.A.* **107**, 856–861
- Sawamiphak, S., Seidel, S., Essmann, C. L., Wilkinson, G. A., Pitulescu, M. E., Acker, T., and Acker-Palmer, A. (2010) *Nature* **465**, 487–491
- Shibuya, M. (2006) *J. Biochem. Mol. Biol.* **39**, 469–478
- Takahashi, T., Yamaguchi, S., Chida, K., and Shibuya, M. (2001) *EMBO J.* **20**, 2768–2778
- Kou, R., SenBanerjee, S., Jain, M. K., and Michel, T. (2005) *Biochemistry* **44**, 15064–15073
- Wu, L. W., Mayo, L. D., Dunbar, J. D., Kessler, K. M., Baerwald, M. R., Jaffe, E. A., Wang, D., Warren, R. S., and Donner, D. B. (2000) *J. Biol. Chem.* **275**, 5096–5103
- Waltenberger, J., Claesson-Welsh, L., Siegbahn, A., Shibuya, M., and Heldin, C. H. (1994) *J. Biol. Chem.* **269**, 26988–26995
- Zhang, Q., Wang, D., Kundumani-Sridharan, V., Gadiparthi, L., Johnson, D. A., Tigyi, G. J., and Rao, G. N. (2010) *Blood* **116**, 1377–1385
- Lehman, N., Di Fulvio, M., McCray, N., Campos, I., Tabatabaian, F., and Gomez-Cambronero, J. (2006) *Blood* **108**, 3564–3572
- Gorshkova, I., He, D., Berdyshev, E., Usatuyk, P., Burns, M., Kalari, S., Zhao, Y., Pendyala, S., Garcia, J. G., Pyne, N. J., Brindley, D. N., and Narayanan, V. (2008) *J. Biol. Chem.* **283**, 11794–11806
- Kramer, K. L., Barnette, J. E., and Yost, H. J. (2002) *Cell* **111**, 981–990
- Wouters, M. M., Roeder, J. L., Tharayil, V. S., Stanich, J. E., Strega, P. R., Lei, S., Bardsley, M. R., Ordog, T., Gibbons, S. J., and Farrugia, G. (2009) *J. Biol. Chem.* **284**, 21177–21184
- Herbert, S. P., Odell, A. F., Ponnambalam, S., and Walker, J. H. (2009) *J. Biol. Chem.* **284**, 5784–5796
- Herbert, S. P., and Walker, J. H. (2006) *J. Biol. Chem.* **281**, 35709–35716
- Needleman, P., Turk, J., Jakschik, B. A., Morrison, A. R., and Lefkowitz, J. B. (1986) *Annu. Rev. Biochem.* **55**, 69–102
- Szymczak, M., Murray, M., and Petrovic, N. (2008) *Blood* **111**, 3514–3521
- Connor, K. M., SanGiovanni, J. P., Lofqvist, C., Aderman, C. M., Chen, J., Higuchi, A., Hong, S., Pravda, E. A., Majchrzak, S., Carper, D., Hellstrom, A., Kang, J. X., Chew, E. Y., Salem, N., Jr., Serhan, C. N., and Smith, L. E. (2007) *Nat. Med.* **13**, 868–873
- Cheranov, S. Y., Karpurapu, M., Wang, D., Zhang, B., Venema, R. C., and Rao, G. N. (2008) *Blood* **111**, 5581–5591
- Chava, K. R., Karpurapu, M., Wang, D., Bhanoori, M., Kundumani-Sridharan, V., Zhang, Q., Ichiki, T., Glasgow, W. C., and Rao, G. N. (2009) *Arterioscler. Thromb. Vasc. Biol.* **29**, 809–815
- Rao, G. N., Lassègue, B., Alexander, R. W., and Griendling, K. K. (1994) *Biochem. J.* **299**, 197–201
- Karpurapu, M., Wang, D., Singh, N. K., Li, Q., and Rao, G. N. (2008) *J. Biol. Chem.* **283**, 26577–26590
- Connor, K. M., Krah, N. M., Dennison, R. J., Aderman, C. M., Chen, J., Guerin, K. I., Sapienza, P., Stahl, A., Willett, K. L., and Smith, L. E. (2009) *Nat. Protoc.* **4**, 1565–1573
- Schlessinger, J. (2000) *Cell* **100**, 293–296
- Yeh, M., Gharavi, N. M., Choi, J., Hsieh, X., Reed, E., Mouillessaux, K. P., Cole, A. L., Reddy, S. T., and Berliner, J. A. (2004) *J. Biol. Chem.* **279**, 30175–30181
- Banno, Y., Takuwa, Y., Akao, Y., Okamoto, H., Osawa, Y., Naganawa, T., Nakashima, S., Suh, P. G., and Nozawa, Y. (2001) *J. Biol. Chem.* **276**, 35622–35628
- Dempsey, E. C., Newton, A. C., Mochly-Rosen, D., Fields, A. P., Reyland, M. E., Insel, P. A., and Messing, R. O. (2000) *Am. J. Physiol. Lung Cell. Mol. Physiol.* **279**, L429–L438
- Leslie, C. C. (1997) *J. Biol. Chem.* **272**, 16709–16712
- Suram, S., Gangelhoff, T. A., Taylor, P. R., Rosas, M., Brown, G. D., Bonventre, J. V., Akira, S., Uematsu, S., Williams, D. L., Murphy, R. C., and Leslie, C. C. (2010) *J. Biol. Chem.* **285**, 30676–30685
- Makanya, A. N., Hlushchuk, R., and Djonov, V. G. (2009) *Angiogenesis* **12**, 113–123
- Kubota, S., and Takigawa, M. (2007) *Angiogenesis* **10**, 1–11
- Kerbel, R. S. (2008) *N. Engl. J. Med.* **358**, 2039–2049
- Pechan, P., Rubin, H., Lukason, M., Ardinger, J., DuFresne, E., Hauswirth, W. W., Wadsworth, S. C., and Scaria, A. (2009) *Gene Ther.* **16**, 10–16
- Aiello, L. P., Pierce, E. A., Foley, E. D., Takagi, H., Chen, H., Riddle, L., Ferrara, N., King, G. L., and Smith, L. E. (1995) *Proc. Natl. Acad. Sci. U.S.A.* **92**, 10457–10461
- Skoura, A., Sanchez, T., Claffey, K., Mandala, S. M., Proia, R. L., and Hla, T. (2007) *J. Clin. Invest.* **117**, 2506–2516
- Cheranov, S. Y., Wang, D., Kundumani-Sridharan, V., Karpurapu, M., Zhang, Q., Chava, K. R., and Rao, G. N. (2009) *Blood* **113**, 6023–6033
- Bajpai, A. K., Blaskova, E., Pakala, S. B., Zhao, T., Glasgow, W. C., Penn, J. S., Johnson, D. A., and Rao, G. N. (2007) *Invest. Ophthalmol. Vis. Sci.* **48**, 4930–4938
- Michaelis, U. R., Xia, N., Barbosa-Sicard, E., Falck, J. R., and Fleming, I. (2008) *Invest. Ophthalmol. Vis. Sci.* **49**, 1242–1247
- Barnett, J. M., McCollum, G. W., and Penn, J. S. (2010) *Invest. Ophthalmol. Vis. Sci.* **51**, 1136–1142
- Zhao, T., Wang, D., Cheranov, S. Y., Karpurapu, M., Chava, K. R., Kundumani-Sridharan, V., Johnson, D. A., Penn, J. S., and Rao, G. N. (2009) *J. Lipid Res.* **50**, 521–533
- Guma, M., Rius, J., Duong-Polk, K. X., Haddad, G. G., Lindsey, J. D., and Karin, M. (2009) *Proc. Natl. Acad. Sci. U.S.A.* **106**, 8760–8765